



HAL
open science

Combining spatial modeling tools and biological data for improved multispecies assessment in restoration areas

Céline Clauzel, Claire Godet

► To cite this version:

Céline Clauzel, Claire Godet. Combining spatial modeling tools and biological data for improved multispecies assessment in restoration areas. *Biological Conservation*, 2020, 250, pp.108713. 10.1016/j.biocon.2020.108713 . halshs-02913473

HAL Id: halshs-02913473

<https://shs.hal.science/halshs-02913473v1>

Submitted on 17 Oct 2022

HAL is a multi-disciplinary open access archive for the deposit and dissemination of scientific research documents, whether they are published or not. The documents may come from teaching and research institutions in France or abroad, or from public or private research centers.

L'archive ouverte pluridisciplinaire **HAL**, est destinée au dépôt et à la diffusion de documents scientifiques de niveau recherche, publiés ou non, émanant des établissements d'enseignement et de recherche français ou étrangers, des laboratoires publics ou privés.



Distributed under a Creative Commons Attribution - NonCommercial 4.0 International License

Title page

Combining spatial modeling tools and biological data for improved multispecies assessment in restoration areas.

Céline Clauzel¹, Claire Godet¹

¹ LADYSS UMR 7533 CNRS, Université de Paris, 75013 Paris, France

Corresponding author : Céline CLAUZEL

1 Combining spatial modeling tools and biological data for improved 2 multispecies assessment in restoration areas

4 Highlights

- 5 - Habitat restoration or creation is one of the actions to reduce fragmentation
- 6 - Our goal was to improve multiscale and multispecies functional connectivity.
- 7 - We modeled habitat suitability and ecological network for eight pond-dwelling species.
- 8 - Forest edges appeared strategic for improving multispecific connectivity.
- 9 - The results provide insights into central issues of biodiversity offset and habitat restoration.

11 Abstract

12 Habitat restoration is one of the actions to reduce landscape fragmentation by promoting connectivity and
13 thus biodiversity. But knowing where to implement these habitats is a major issue and planners lack
14 guidance for answering this question, in particular when it involves multiple species and over a large area.
15 We proposed to combine biological data, habitat suitability models and spatial graphs to improve
16 multiscale and multispecies connectivity in Ile-de-France, a highly artificialized region of 12,000 km². The
17 framework consisted of i) modeling habitat suitability for eight pond-dwelling species (*Alytes obstetricans*,
18 *Bufo bufo*, *Epidalea calamita*, *Hyla arborea*, *Rana temporaria*, *Salamandra salamandra*, *Triturus*
19 *cristatus*, and *Natrix natrix*), ii) modeling the ecological network for each species, iii) prioritizing each
20 sampling point depending on the gain in connectivity if a new pond was created there and iv) combining
21 single-species results to identify the areas that could improve multispecies connectivity. The multivariate
22 statistical analysis revealed that transitional forest environments appeared to be the most strategic areas for
23 improving multispecific connectivity (at least for 5 species). Targeted addition of habitat within an
24 ecological network can increase habitat density in deficient areas and reconnect network sub-parts. This
25 approach is therefore promising to guide conservation actions and “no net loss” biodiversity measures,
26 especially the final stage of offset in the mitigation hierarchy.

29 **Keywords:** multispecies approach, amphibian, habitat suitability models, landscape graph, functional
30 connectivity, biodiversity offset

33 1. Introduction

34 Urbanization and agricultural intensification lead to a reduction and a fragmentation of natural and semi-
35 natural habitats. Wetlands and ponds have particularly been affected, experiencing a global 70% decrease
36 since the beginning of the 20th century (Davidson, 2014). This reduction has direct consequences on the
37 viability of animal populations. Among the current mass extinction of biodiversity, amphibian and reptile
38 species are recognized as the most threatened vertebrate group. According to the International Union for
39 Conservation of Nature (IUCN), more than half (59%) of amphibians and 42% of reptiles are declining
40 worldwide. These trends are probably underestimated because a large proportion of species (23%) are “data

41 deficient” and are not integrated into population trend analyses (Howard and Bickford, 2014). The drivers
42 of this decline are mostly related to human activities, habitat loss and landscape fragmentation, as well as
43 environmental pollutants, infectious diseases and global climate change (Hayes et al., 2010). Their
44 vulnerability is notably due to their biphasic life cycle, which induces many movements between aquatic
45 and terrestrial habitats.

46 Many studies have documented this extinction crisis and proposed conservation actions mostly related to
47 protected area design, sustainable conservation measures, species translocation or habitat
48 restoration/creation (Godet and Devictor, 2018). Since many amphibians can live in artificial wetlands and
49 ponds, habitat restoration and even the creation of new ponds could be an effective solution to reduce
50 landscape fragmentation. But Grant et al. (2019) noted that species conservation, especially amphibian
51 conservation, had failed. They advocate an improved complementarity between research and management
52 to increase the effectiveness of conservation actions. For example, in the case of amphibian populations
53 living in fragmented habitats and highly dependent on fluxes between patches (Hanski and Ovaskainen,
54 2000), aquatic habitat restoration should integrate both local-scale factors such as microtopography, water
55 quality or nearby terrestrial habitat and broad-scale factors such as connectivity between habitats (Hodgson
56 et al., 2011) to maintain regional connections and, consequently, the viability of populations (Briers, 2002;
57 Moilanen et al., 2005). If expert opinions and field data could provide information about local-scale factors,
58 then their large-scale generalization would be complex due to the large amount of data required. In
59 addition, landscape managers lack information on where to restore future habitats, how many and how to
60 arrange them, e.g., many habitats close together or habitats scattered to cover a large area (Schmidt et al.,
61 2019). Recently, several studies have attempted to answer these questions by performing dynamic models
62 (Scroggie et al., 2019) or connectivity models (Clauzel et al., 2015; Jeliaskov et al., 2019; Matos et al.,
63 2019). Despite promising results for conservation actions, these studies focused on a single species.
64 Designing a method to target restoration areas depending on regional connectivity for multiple species is
65 still challenging.

66 We hypothesized that bringing together field expertise (expert opinion and biological data) and spatial
67 modeling tools (prediction and simulation) could fill this gap. Several studies have been published on
68 multispecies assessment of connectivity to prioritize core habitats and corridors (Khosravi et al., 2018;
69 Lechner et al., 2017; Meurant et al., 2018), to reduce road fragmentation (Mimet et al., 2016; Santini et al.,
70 2016) and to quantify the impacts of land cover changes (Sahraoui et al., 2017). But to our knowledge, no
71 studies have implemented it on the assessment of habitat restoration, which is a major challenge for
72 biodiversity conservation. We proposed to combine habitat suitability models and landscape graphs to take
73 advantage of their respective strengths and partially overcome their limitations. Graph-based modeling is a
74 widely used method for analyzing connectivity in habitat networks (Dale and Fortin, 2010; Foltête, 2019;
75 Galpern et al., 2011; Minor and Urban, 2008; Urban et al., 2009). Landscape graphs are considered
76 spatially explicit models of ecological networks designed from both environmental and biological data.
77 Similar to any spatial graph (Fall et al., 2007), landscape graphs constitute a mathematical object on which
78 connectivity metrics can be calculated at different levels (Rayfield et al., 2011). These metrics provide
79 indicators for prioritizing habitats to preserve, assessing the potential impact of land-use changes and
80 identifying the best locations to restore habitats or corridors (Foltête, 2019). However, like any modeling
81 method, landscape graphs also have limitations, especially regarding the reliance of the representation of
82 the actual habitat network (Moilanen, 2011). One solution to improve this limitation is to incorporate
83 biological data in graph modeling through habitat suitability models (HSMs). Based on the concept of
84 ecological niche, a HSM predicts species potential distribution by analyzing and extrapolating the statistical
85 relation between species presence and environmental variables (Guisan and Zimmermann, 2000). The
86 resulting HSM maps allow the identification of the most suitable areas for habitat patches. However, they
87 cannot provide information about the connections between these suitable areas, for which a connectivity
88 analysis is required. Combining HSM and landscape graphs has already been performed using various
89 alternative techniques and input data for a single species (Almpanidou et al., 2014; Clauzel et al., 2013;
90 Decout et al., 2012; Dufлот et al., 2018; Schank et al., 2020; Ziólkowska et al., 2012). In most cases, HSM

91 has been used to define both habitat patches and least-cost paths, thus mixing two different ecological
 92 processes, habitat selection and movement, which may be a questionable practice. Radio-telemetry data
 93 (Ziółkowska et al., 2012) or individual-based simulations (Coulon et al., 2015) appear relatively more
 94 relevant but require complex data that are difficult to collect for several species and over a wide area.
 95 Furthermore, GPS data provide information on actual movements but not on alternative routes that could be
 96 used in case of disturbance. To overcome these difficulties, we used HSM to delineate optimal habitat
 97 patches as well as previous field experimentations combined with expert opinions to calibrate least-cost
 98 paths from a resistance landscape map.

99 We applied this protocol to the simultaneous conservation of eight species to search for the best locations
 100 for pond creation, i.e., optimizing connectivity for as many species as possible. The analysis was applied in
 101 the Ile-de-France region (France), a highly disturbed region, which is poorly represented in dispersal
 102 studies that tend to occur in less disturbed semi-natural habitats (Bailey and Muths, 2019).

103

104 2. Materials & Methods

105 2.1. Study area and studied species

106 The study area (12,000 km²) is the administrative region of Ile-de-France surrounding the city of Paris
 107 (France) (48.6°N; 3.2°E). The landscape is dominated by intensive agriculture (50%), urbanized areas
 108 (24.5%) and forests (24%). Water bodies and rivers occupy only 1.5% of the area (IAU, 2019). The Ile-de-
 109 France region is home to 12 reptile species and 17 amphibian species (Zucca et al., 2019). The species
 110 under study were selected according to several criteria: ponds as one of the habitats, sufficient occurrence
 111 data, various optimal habitat types and various dispersal abilities between species. Species occurrence data
 112 were extracted from the naturalist database CETTIA, which has included both protocolled and opportunistic
 113 data at the regional level since 2012. Eight species with distinct ecological preferences were retained: 7
 114 amphibians (*Alytes obstetricans*, *Bufo bufo*, *Epidalea calamita*, *Hyla arborea*, *Rana temporaria*, *Triturus*
 115 *cristatus*, and *Salamandra salamandra*) and 1 reptile (*Natrix natrix*). Literature including naturalist guides
 116 (Bensettiti and Gaudillat, 2004 ; Grand et al., 2014 ; Lescure and Massary, 2012), regional studies
 117 (Sordello et al., 2011) and scientific studies (Sahraoui et al., 2017) helped us to identify the ecological
 118 characteristics of the species in terms of aquatic and terrestrial habitats, environments favorable or
 119 unfavorable to movement and daily and annual movement capacity. Some species are specialized more
 120 than others with a preference for either forest ponds or open-area ponds. Some tolerate artificial
 121 environments such as quarries or sandpits, while others avoid them (Table 1). Their dispersal abilities vary
 122 from 100 m for *S. salamandra* to 9,000 m for *R. temporaria*.

123

124 Table1 – General species’ ecology, freshwater habitat types, number of occurrence data in CETTIA
 125 database, daily and dispersal distances for each of the eight species under study, based on information from
 126 the literature.

General species’ ecology	Preferred freshwater habitat type	Species	Number of observations in CETTIA database	Maximum dispersal distance	Daily movement
Can use different kind of ponds, including large bodies of water	Ponds and all water surfaces	<i>Bufo bufo</i>	9,608	2,500 m	200 m
Dependent on a network of varied types of ponds	Ponds	<i>Hyla arborea</i>	372	4,000 m	500 m
Dependent on low-density forest, shrublands, and grasslands	Ponds in or near the forest	<i>Natrix natrix</i>	750	3,000 m	200 m
		<i>Rana temporaria</i>	1,038	9,000 m	200 m

Dependent of forest	Ponds in or near the forest	<i>Salamandra salamandra</i>	130	100 m	50 m
Dependent on open environments and temporary ponds. Tolerant of artificial environments (quarry and sandpit)	All ponds, except those in forest cores	<i>Epidalea calamita</i>	322	2,500 m	200 m
Dependent on open environments. Urban areas tolerant		<i>Alytes obstetricans</i>	413	150 m	100 m
Dependent of open and shrubby environments and on a dense network of ponds		<i>Triturus cristatus</i>	485	1,000 m	100 m

127

128 2.2. Habitat suitability modeling

129 For each species, habitat suitability was modeled by linking occurrence records, which varied from 130
130 points for *S. salamandra* and 9,608 for *B. bufo*, and a set of environmental variables. These predictive
131 variables were chosen according to their potential ecological relevance for pond-dwelling species (Wilson
132 et al., 2013). Thirteen variables corresponding to four different data categories were selected (Table 2).
133 Two topographic variables (slope and roughness) were obtained from the digital elevation model of the Ile-
134 de-France provided by IGN. Temperatures were extracted from BIOCLIM data derived from MODIS LST
135 reconstructed at a resolution of 250 m pixels (Metz et al., 2014) and precipitations from CHELSEA
136 (climatologies at high resolution for the earth's land surface areas) data (Karger et al., 2017). The NDVI
137 (normalized difference vegetation index) was obtained from Landsat 8 satellite images. Landscape and
138 proximity variables described the habitat quality of the pixel neighborhood (availability of daily resources
139 or local disturbances). As the extent of this neighborhood could be different depending on the ecology of
140 the species, three radius buffers were selected to calculate the percentage area of the land cover categories.
141 Landscape and proximity variables were calculated from a landscape map built from the combination of
142 three databases: i) the Ile-de-France's land use produced by the L'Institut Paris Region, ii) the BD TOPO@
143 IGN for linear landscape elements such as roads and rivers and iii) the pond database of the National
144 Society for the Protection of Nature. The resulting landscape map had 17 categories (Appendix A) and was
145 rasterized at a 10 m resolution.

146 Table 2. Description and sources of the 13 environmental variables used for modeling habitat suitability of
147 each species

Category	Variable	Resolution	Data source
Bioclimatic	NDVI	30 m	Landsat 8 (layers band 5 et band 4) NDVI = (NIR - R)/(NIR+R) August 2019
	Temperatures	250 m	BIOCLIM data derived from MODIS LST
	Precipitations	1 km	Chelsea (Climatologies at high resolution for the earth's land surface areas)
Topographic	Slope	25 m	MNT
	Roughness	25 m	MNT
Landscape composition with a buffer size of 50 m; 200 m; 500 m	Forest	10 m	Landscape map
	Grassland	10 m	Landscape map
	Quarry	10 m	Landscape map
	Water	10 m	Landscape map
	Artificial areas	10 m	Landscape map
Proximity	Distance to the nearest road	10 m	Landscape map
	Distance to the nearest river	10 m	Landscape map
	Distance to the nearest pond	10 m	Landscape map

148

149 Habitat suitability modeling was performed with MaxEnt (Phillips et al., 2017), an open-source software
150 based on the maximum-entropy approach for modeling species niches and distributions. To avoid potential
151 bias (Fourcade et al., 2014; Kramer-Schadt et al., 2013), we analyzed the data set before modeling to check
152 for inconsistencies or outliers. We then removed duplicates in each 10mx10m resolution cell so that there
153 were no overestimates in some places. We maintained the default settings that are recognized to perform as
154 well as the adjusted settings (Phillips and Dudík, 2008). Models were replicated ten times, and the average
155 probabilities of predicted presence were retained for further analysis. The robustness of the models was
156 examined using a *k*-fold cross-validation procedure, wherein species presence points are randomly split into
157 *k* equal-sized subsets to successively serve as test data, while the remaining *k*-1 folds are used as training
158 data (Guisan and Zimmermann, 2000). Prediction performance is related to the error rate
159 (misclassification) of the test data, which is measured by the extrinsic omission rate and the area under the
160 curve (AUC) (Guisan and Zimmermann, 2000). AUC is a threshold-independent standard measure of
161 model accuracy that ranges from 0 to 1. It can be interpreted as the probability that a randomly chosen
162 species presence point will be correctly classified by the model (Phillips et al., 2006). Maxent indicates
163 which variables most contribute to the presence of each species and what the shape the relationship is. As a
164 result, the habitat suitability maps were created by applying each species distribution model to all cells in
165 the study area using a logistic function to obtain a habitat suitability index (HSI) ranging from 0 to 1
166 (Phillips and Dudík, 2008).

167 *2.3. Landscape graph construction*

168 From each habitat suitability map, corresponding to the presence probability of each species, a landscape
169 graph, composed of a set of habitat patches (nodes) potentially connected by links, was built at the
170 dispersal scale. Habitat patches were defined as the highest values of habitat suitability (Dufлот et al.,
171 2018). The threshold value used corresponded to the maximum sum of sensitivity and specificity (Max
172 SSS) (Liu et al., 2013) and could be different according to the species. Habitat patches were associated with
173 an attribute representing their potential quality for pond-dwelling species. As the habitat patches derived
174 from the HSI map could include both aquatic and terrestrial environments, the quality was determined by
175 multiplying the area of the patch by its average HSI value.

176 The links of the graph were defined in a complete topology, i.e., all the links between patches were
177 potentially taken into account. Their impedance was calculated in cost distances based on a resistance map.
178 From a previously constructed landscape map, each category was classified according to its resistance to
179 species movement, using the ecological literature and local experts' opinions (see Appendix A for all the
180 resistance values for each species). Habitat patches, i.e., the highest habitat suitability values, were assigned
181 a resistance of 1. The favorable landscape elements were assigned a low value (10), neutral elements a
182 value of 100, unfavorable elements a value of 1,000, and barrier elements the highest value (10,000). This
183 logarithmic scale was chosen based on several studies (Clauzel et al., 2013; Verbeylen et al., 2003) that
184 have shown the importance of contrasting resistance values between favorable and unfavorable elements to
185 explain the presence of species. These resistance values were then submitted to several experts in
186 herpetology, who allowed the values to be refined according to the local characteristics of the landscape
187 and/or the species. Only the links with distances shorter than the dispersal capacity of the species were
188 retained. Each resulting graph thus represented the potential ecological network of a species, taking into
189 account the environmental variables that best explain its presence in the Ile-de-France region.

190 *2.4. Patch addition process*

191 The graphs constructed in the previous step were used to identify the best locations for pond creation. We
192 applied the method developed by Clauzel et al. (2015) and Mimet et al. (2016). The method consists of (1)
193 calculating a global metric quantifying the initial connectivity of the network, (2) applying a sampling grid
194 of a given resolution to the study area and then (3) evaluating the potential contribution of each centroid of
195 cells by quantifying the increase in the connectivity index provided by the addition of a new node and of

196 new potential links from this node to other existing nodes (Fig. 1). After testing all the cells, the algorithm
197 validated the one for which patch addition produced the largest increase in the metric value.

198 The global connectivity metric to be maximized was the Equivalent Connectivity (EC) index, defined as
199 the “amount of reachable habitat” for a species at the landscape scale (Saura et al., 2011):

$$200 \quad EC = \sqrt{\sum_{i=1}^n \sum_{j=1}^n a_i a_j P_{ij}^*}$$

201 where n is the number of nodes, a_i is the attribute of node i , a_j is the attribute of node j and P_{ij}^* is the
202 maximum probability of all potential paths between nodes i and j . P_{ij} is determined by an exponential
203 function such that:

$$204 \quad P_{ij} = e^{-\alpha d_{ij}}$$

205 where d_{ij} is the least-cost distance between these nodes and α is a constant expressing the intensity of the
206 decrease in the probability of movement (p) with distance (d). As d corresponded to the dispersal distance,
207 the setting of the metric was specific to each species.

208 Running these calculations (graph construction and patch addition process) over the whole region was very
209 time consuming and not necessarily ecologically relevant. We therefore choose to limit the connectivity
210 analysis to a 150 km² subpart for the demonstration. The patch addition process was applied on a sampling
211 grid of 15,093 points evenly spaced 100 m apart.

212 The landscape graph construction and the patch addition method were performed using Graphab 2.4
213 software (Foltête et al. 2012; see <http://thema.univ-fcomte.fr/productions/graphab/>).

214 *2.5. From single-species to multispecies connectivity improvement*

215 The protocol described above was used to calculate the connectivity gain G_{ki} from each location tested k
216 and for each species i . A multivariate analysis was then performed to identify the best locations for creating
217 a new pond with a multispecies approach, i.e., optimizing connectivity for as many species as possible. The
218 values of G_{ki} were grouped in a table and processed in a principal component analysis (PCA). To obtain a
219 sufficiently satisfactory approximation, we used eigenvalues to determine the number of principal
220 components to be retained (Kaiser, 1961) and the graph of eigenvalues (scree plot). The number of axes
221 was determined by the point beyond which the remaining eigenvalues were all relatively small and of
222 comparable size (Jolliffe, 2002; Peres-Neto et al., 2005).

223 We also performed cluster analysis on the observations, i.e., for each of the 15,093 cells of the grid to
224 group together points that had similar values of G_{ki} using the *k-means* classification algorithm. From an
225 ecological point of view, this allows to identify which species could benefit at the same time from the
226 creation of a same pond. The appropriate number of clusters was determined by the elbow method. It
227 consisted of plotting the explained variance as a function of the number of clusters and picking the elbow
228 of the curve as the number of clusters to use. A Kruskal-Wallis test was then used to study the variations in
229 the species abundance between the different clusters. Subsequent post hoc pairwise Wilcoxon rank sum test
230 was carried out to reveal the differences between each pair of clusters regarding the values of G_{ki} of each
231 species.

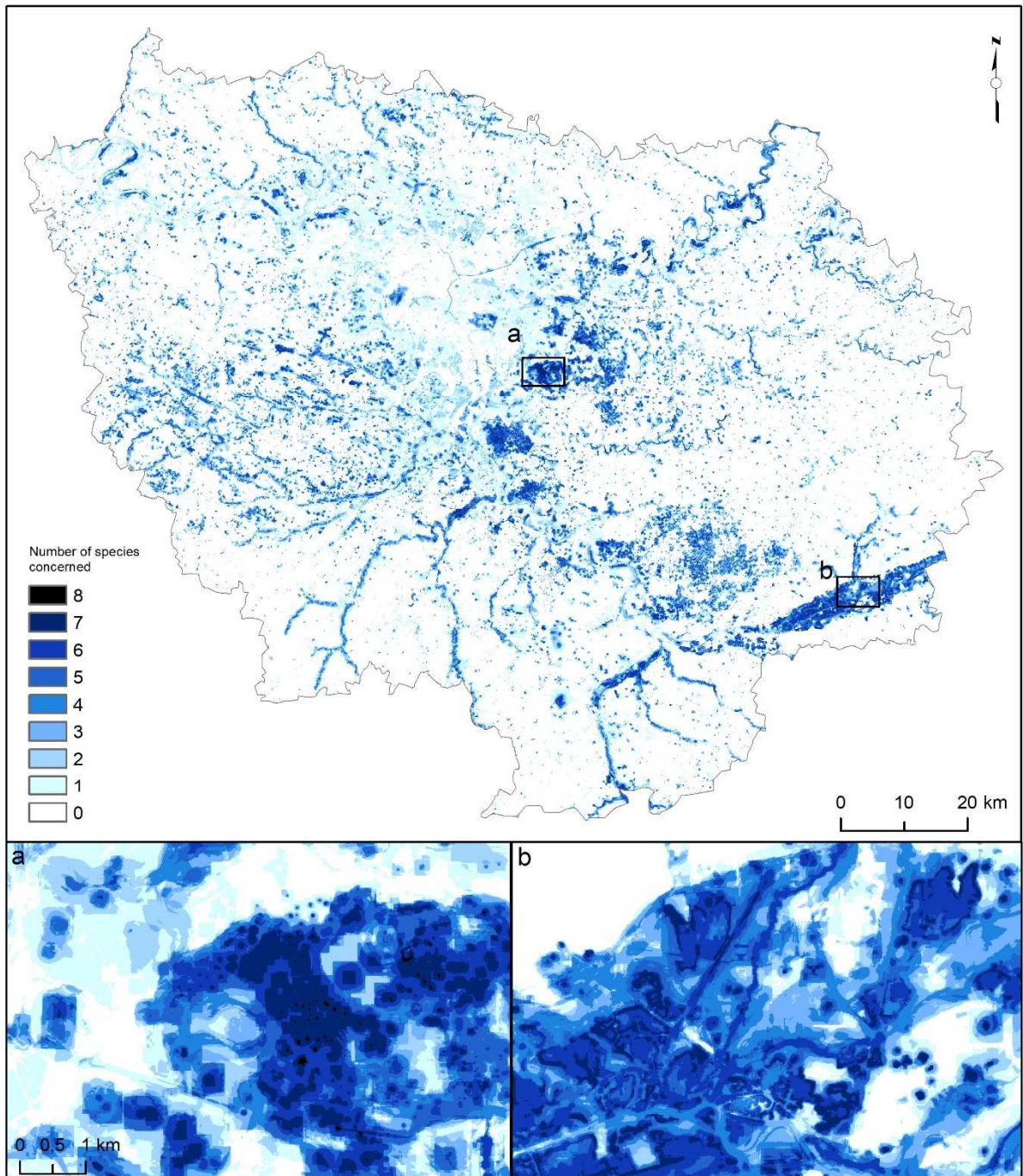
232

233 **3. Results**

234 *3.1. Habitat suitability models (HSM) and significant environmental variables*

235 For each species, the variables were selected from a collinearity study (<70%) and the contribution of the
236 variables in an HSM for each species, including all environmental variables. A 10-fold cross-validation
237 procedure indicated good models for our studied eight species (see Appendix B, AUC > 0.7). In most
238 cases, “distance to the nearest ponds” and “water surface area” were logically the environmental variables
239 that contributed most to the best predictive model (Appendix C). Distance to the nearest pond was
240 negatively correlated with the presence of *T. cristatus* (an average contribution of 69.5%), *H. arborea*
241 (44.6%), *A. obstetricans* and *R. temporaria* (34.4 and 33%, respectively), *E. calamita* (22%), *N. natrix* and
242 *B. bufo* (15% and 12%). Proportion of the water surface was positively correlated with the presence of *B.*
243 *bufo* (51%), *N. natrix* (36.5%), *R. temporaria* (31%), *S. salamandra* (24%), *H. arborea* (21%), *A.*
244 *obstetricans* (16%), and *T. cristatus* (13%). Some variables were significant only for a few species
245 depending on their ecological preferences, such as the proportion of forests (*S. salamandra* 30.5%, *R.*
246 *temporaria* 27.7%, *B. bufo* 18.6%, and *N. natrix* 16.9%) or the proportion of artificial environments (*A.*
247 *obstetricans* 24.2% and *E. calamita* 14.8%). The first variable was positively correlated with species
248 presence (the greater the proportion of forest, the higher the probability was), while the response of the
249 second variable had a Gaussian form; i.e., only the moderate values were positive (see Appendix C). For all
250 the landscape composition variables, the most significant buffer radius was 500 m for the species except for
251 *A. obstetricans* and *T. cristatus* (200 m). Temperatures were significant only for *E. calamita* (32.1%), for
252 which the probability of presence was a maximum temperature between 12°C and 13.6°C. High annual
253 amounts of precipitation (< 700 mm) were correlated with the presence of *S. salamandra* (17.4%).

254 Given the different responses of the variables between species, the maps of the probability of presence
255 were very different (Appendix D). The proportion of the Ile-de-France region occupied by habitat patches
256 varied according to the species, between 0.55% for *S. salamandra* and 15.30% for *R. temporaria*. The
257 combination of the eight habitat binary maps (Fig. 1) highlighted that 68% of the region had no potential
258 habitat (mainly urban areas and intensive agricultural land), and 14% was habitat for only one species. In
259 addition, 13% of the region (1617 km²) was habitat for 2 to 4 species and 7% (846 km²) for more than 4
260 species. Only 0.002% (0.24 km²) was habitat for all eight species. These areas had a high density of water
261 bodies (ponds, rivers, and wetlands), located either in a few forest massifs (Fig. 1a) or along river valleys
262 such as the southeastern Seine valley (Fig. 1b).



263
 264 Fig. 1: Combination of the eight habitat binary maps extracted from the habitat suitability models. The
 265 colors indicate the number of concerned species by habitat patches.

266
 267 *3.2. Ecological network modeling*

268 From these HSM maps, we selected a subpart of the region based on two criteria: i) the area must contain
 269 optimal habitat for the eight species, ii) habitat must be fragmented so that the creation of a new habitat is
 270 of ecological interest. A complete-topology graph was built for each species by keeping only those links
 271 whose distance was less than the dispersal distance. Connectivity evaluated by the Equivalent Connectivity
 272 metric varied greatly between species (Table 3 and Appendix E). The ecological networks of *B. bufo*, *R.*
 273 *temporaria* and to a lesser extent *N. natrix* had the highest connectivity due to the large area of potential
 274 habitat. The ecological networks of *T. cristatus*, *H. arborea*, *E. calamita* and *A. obstetricans* had seven

275 times less connectivity than those of the other species. Their ecological networks contained fewer habitat
 276 patches and were more fragmented, including that of *A. obstetricans*. *S. salamandra* was the only species
 277 that had extremely low connectivity, as the 16 potential habitat patches were almost all disconnected.

278 *3.3. Improving single-species connectivity*

279 The patch addition process was applied on a sampling grid of 15,093 points evenly spaced 100 m apart to
 280 cover the entire 150 km² regional subpart. The connectivity gain provided by the best locations for the
 281 creation of a new pond was very low overall (< 2%), except for *T. cristatus*, for which the gain reached
 282 38.4% and to a lesser extent for *S. salamandra* (8.6%).

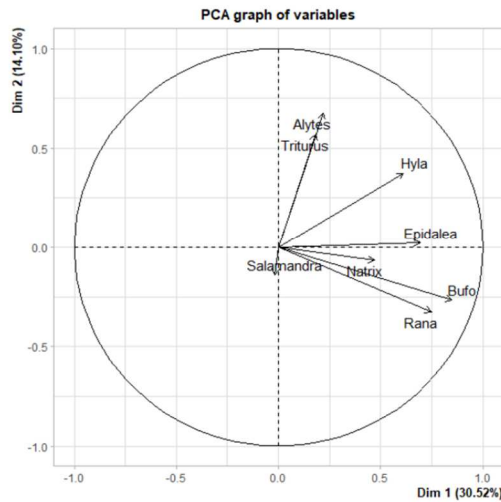
283
 284 Table 3- Initial Equivalent Connectivity (EC) metric (expressed in m²) and the minimum, average and
 285 maximum values of the rate of change (%) in the EC provided by the addition of a new pond in the network
 286 of each species.

Species	Initial EC (m ²)	Rate of change (%)		
		Minimum	Mean	Maximum
<i>Alytes obstetricans</i>	2,328,493	0.00108	0.0148	2.0039
<i>Bufo bufo</i>	17,066,498	0.00054	0.2238	0.3408
<i>Epidalea calamita</i>	1,847,265	0.00042	0.1335	1.5207
<i>Hyla arborea</i>	2,562,923	0.00043	0.0629	1.7516
<i>Natrix natrix</i>	13,797,042	0.00095	0.0731	0.3616
<i>Rana temporaria</i>	16,125,400	0.00029	0.2062	0.2450
<i>Salamandra salamandra</i>	17,265	0.55110	0.5614	8.6042
<i>Triturus cristatus</i>	3,267,325	0.00168	0.1357	38.3911

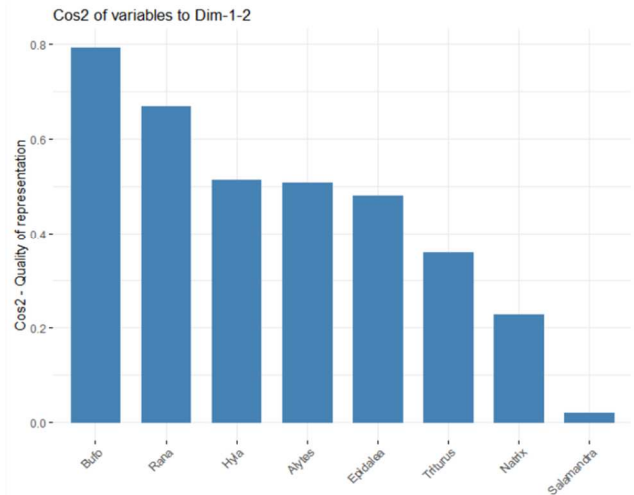
287
 288 *3.4. Improving multispecies connectivity*

289 From the PCA analysis, the first two components explained 45% of the total variance (Table 4). The
 290 species that were best represented by these components were *B. bufo* (80%), *R. temporaria* (65%), *H.*
 291 *arborea*, *A. obstetricans* and *E. calamita* (50%). Only *S. salamandra* was not well represented by the first
 292 two components (Fig. 2b). The first component hierarchized the new pond locations for five species (*R.*
 293 *temporaria*, *B. bufo*, *N. natrix*, *E. calamita*, and *H. arborea*) and the second axis for two species (*A.*
 294 *obstetricans* and *T. cristatus*). The nearly orthogonal arrangement of several species in the PCA (Fig. 2a)
 295 indicated that there was no spatial correspondence in the best locations, and no compromise could be found
 296 to account for the eight species.

A)



B)

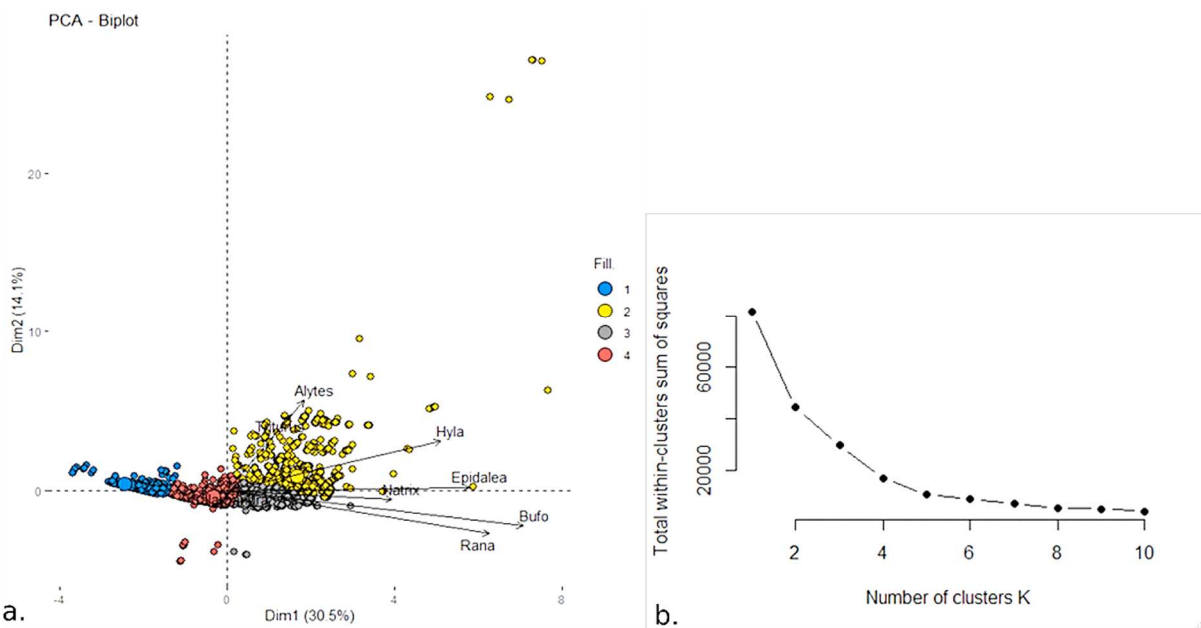


297
 298 Fig 2. – A) The eight species projected onto the planes formed by the first two components of the PCA; B)
 299 histogram of the contribution of each species to the first two components.

300 Table 4. Eigenvalue and amount of variance accounted for by each component of the PCA.

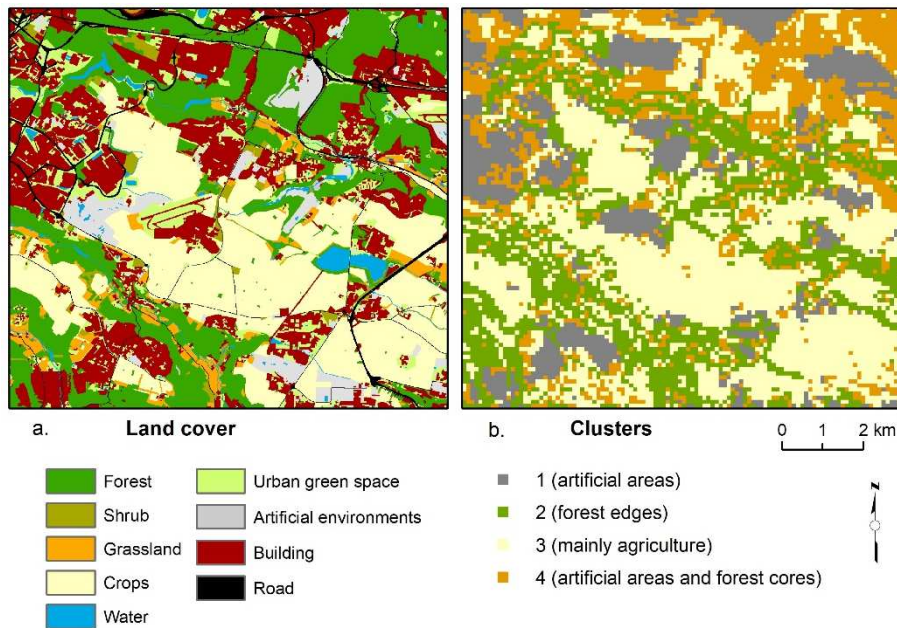
Component	Eigenvalue	% of variance	Cumulative %
1	2.4412414	30.515517	30.51552
2	1.1277741	14.097176	44.61269
3	1.0391739	12.989674	57.60237
4	0.9782465	12.228082	69.83045
5	0.9220738	11.525923	81.35637
6	0.7297676	9.122094	90.47847
7	0.4675788	5.844735	96.32320
8	0.2941439	3.676799	100.00000

301
 302 We classified the 15,093 locations for the new ponds into 4 groups using the *k-means* classification
 303 algorithm (Fig. 3) and spatially projected these clusters on the study area (Fig. 4). The connectivity gain
 304 varied significantly between the clusters for each species (Appendix F). The percentage increase in the EC
 305 was the highest in cluster 2 for most species, except for *B. bufo* and *R. temporaria*, which had their highest
 306 EC value in cluster 3. The landscape of cluster 2 was dominated by forests (43%) but also contained urban
 307 green spaces, artificial areas and cultures (approximately 15% each). The landscape of cluster 3 was
 308 dominated by agriculture (49%), followed by forests (28%) and artificial areas (12%). Cluster 1,
 309 characterized by a strong dominance (89%) of artificial surfaces and urban green spaces (9%), seemed to
 310 have the lowest EC increase values for all species, whereas cluster 4 (containing both artificial areas at 39%
 311 and forests at 34%) had average values for *B. bufo*, *R. temporaria*, *N. natrix* and *E. calamita*.



312 a. 313 Fig. 3. The locations for new ponds were projected in the factorial planes formed by the first two
 314 components of the PCA (a). The colors of the points were related to the four different clusters attributed by
 315 the *k-means* method (b): cluster 1 (artificial areas) ; cluster 2 (forest edges) ; cluster 3 (mainly agriculture) ;
 316 cluster 4 (artificial areas and forest cores).

317



318 319 Fig. 4 – Land cover map of the patch addition area (a) and spatial projection of the four clusters grouping
 320 the 15,093 points according to the connectivity gain for the eight species (b).

321

322 4. Discussion

323 Our approach for restoring habitats prioritized areas based on their contribution to multispecies regional
 324 connectivity. Targeted addition of habitat within an ecological network can increase habitat density in
 325 deficient areas and reconnect network sub-parts. This approach is therefore promising to guide

326 conservation actions and “no net loss” biodiversity measures, especially the final stage of “offset” in the
327 mitigation hierarchy (Ermgassen et al., 2019). Indeed, depending on the structure of the network, it may
328 sometimes be more ecologically relevant to create habitat at a strategic location in the network, rather than
329 necessarily near the habitat destroyed by the project (Bergès et al., 2020). However, managers currently
330 lack information on the contribution of biodiversity offset areas to regional connectivity (Moilanen and
331 Kotiaho, 2018). This involved taking into account the spatio-temporal nesting of ecological processes to
332 propose effective and relevant conservation actions. Among the many studies on amphibian movement that
333 have been published (Pittman et al., 2014; Smith and Green, 2005), most are focused on a single scale and
334 life stage (habitat use, migration or dispersal), and very few have tried to integrate multiple spatial scales
335 (Bailey and Muths, 2019). The modeling of ecological networks based on graph theory included both daily
336 movements, through the definition of the patch quality, and dispersal events in maximizing the connectivity
337 metric. Furthermore, the same protocol can be applied to other scales depending on the ecological process
338 (e.g., seasonal migrations, range shifts related to climate change) we want to support through habitat
339 restoration. Here, we focused on connectivity at the dispersal scale, using the global metric EC, which
340 integrates both the amount of habitat and the degree of connections between habitat patches. Selecting this
341 metric to optimize allowed us to take into account both the gain in local connectivity through additional
342 habitat area and in regional connectivity through connections at the dispersal scale. Habitat restoration in
343 areas with high connectivity gains could therefore enhance existing local populations and promote
344 colonization of new habitats (Bailey and Muths, 2019). However, connectivity values should be analyzed
345 in relation to the network configuration to recommend the most appropriate measures for the conservation
346 of the species under study. Indeed, low gains in connectivity may correspond to radically different
347 connectivity situations. The first situation related to very well-connected ecological networks with a high
348 density of habitat patches and connections, such as that for *B. bufo*, *R. temporaria* or *E. calamita*. In this
349 case, adding a new pond would only marginally improve an already high level of regional connectivity. In
350 contrast, another connectivity situation may also correspond to a highly fragmented ecological network,
351 either due to a low density of habitat (e.g., *S. salamandra*) or due to an unfavorable landscape matrix
352 separating main habitat areas (e.g., the central part of the networks of *H. arborea* and *N. natrix*). In these
353 two situations, adding a unique pond is not enough to significantly improve regional connectivity.
354 Nevertheless, in the latter case, adding several ponds cumulatively, as in Clauzel et al. (2015), could
355 reconnect the two main subparts of the network and thus greatly improve connectivity. The proposed
356 protocol can therefore not only provide indications on where to restore a habitat but also on how many
357 habitats in order to significantly improve connectivity, or to restore the original state of connectivity
358 destroyed by a development project.

359 A major challenge for modeling is to build models that are realistic and robust enough to propose relevant
360 conservation actions. This point is crucial and involves the integration of species observation data
361 (presence, abundance, genetic diversity, etc.) into modeling. However, a recent review (Foltête et al., 2020)
362 showed that among the large number of graph-based connectivity studies, very few articles used biological
363 data in combination with landscape graphs. This scenario is probably related to the difficulty in obtaining
364 relevant data, especially when studies involve multiple species and a large area. For example, in Clauzel et
365 al. (2015), the ecological network of *H. arborea* was modeled from occurrence data to retain only occupied
366 ponds as the graph nodes and not all potential habitats, as it is often the case in graph-based connectivity
367 studies. However, this study was applied to a region of 4,000 km² and focused on a single species.
368 Recently, Jeliakov et al. (2019) integrated occurrence data for three amphibian species for an area of 430
369 km² and a set of environmental variables to provide information about structural and functional
370 connectivity on several scales but without providing management recommendations. In our framework,
371 occurrence data of each species was confronted with environmental variables to predict habitat suitability
372 and to delineate optimal habitat patches. This part of the results is interesting in itself for biodiversity
373 conservation because it allows managers to detect – and preserve – shared habitats or conversely species-
374 specific habitats. The large differences in the potential distribution between species could be explained by
375 the degree of habitat specialization. *R. temporaria*, which is a ubiquitous species, had the widest predicted

376 distribution, with 15.30% of the region classified as potential habitat. Conversely, *S. Salamandra*, a more
377 specialized species with low movement abilities, had the lowest predicted distribution (0.55%), but the
378 small number of observations could have limited the relevance of the model.

379 Finally, the major contribution of our paper is the multispecies assessment of restoration areas. In
380 multispecies connectivity studies, the aggregation of the results between species is still challenging
381 (Meurant et al., 2018). Most of them analyzed the results on a species-by-species basis and eventually
382 combined them by simple spatial overlay. The sum or average of the connectivity values obtained per
383 species provides an overall diagnosis on high connectivity areas but with a risk of giving more weight to
384 species that already have a well-connected network. By normalizing the values beforehand, more weight is
385 given to species with rare habitats, which may be consistent with biodiversity conservation objectives
386 (Sahraoui et al., 2017). However, in any case, knowing precisely which species is more concerned is made
387 impossible by these combinations. Here, we combined the results with a multivariate statistical analysis to
388 potentially identify different clusters, i.e., sets of points where connectivity gains are close for some
389 species. This method allowed to identify more robustly the restoration areas that were simultaneously
390 strategic for species that do not have the same ecological network or movement capabilities. If our results
391 revealed that no area seemed to benefit all species, the landscapes dominated by forests and located near
392 agricultural land (cluster 2) were the most strategic area for improving multispecific connectivity (at least
393 for 5 species). Secondly, areas dominated by agriculture appeared to be more suitable for habitat restoration
394 for *B. bufo* and *R. temporaria* (cluster 3).

395

396 5. Conclusions

397 By coupling biological data, habitat suitability models and spatial graphs, the described method in this
398 paper appears to be useful for targeting habitat restoration areas that would simultaneously benefit several
399 species. Integrating functional connectivity into this research increases the probability of colonization of
400 the new habitat as well as potentially reconnecting isolated habitats and thereby improving the robustness
401 and the resilience of the ecological network. The value of this method goes beyond the creation of ponds
402 and can be applied to any type of habitat that can be the subject of restoration measures or a complete
403 creation. The results provide insights into central issues of biodiversity offset and habitat restoration
404 (Moilanen and Kotiaho, 2018): where and how many new habitats should be created to optimize
405 connectivity for multiple species with various movement abilities and within different habitats.

406

407 Acknowledgements

408 The authors thank Carole Gaber (funded by ARP-Astrance in 2018-2019) for her preliminary work on
409 pond-dwelling species and advice. This study was funded by the Ile-de-France Region (TRAMARE project
410 2019-2020). Computations were performed on the TGIR Huma-num server (<https://www.huma-num.fr>).
411 The manuscript was improved by comments from the two anonymous reviewers.

412 References

- 413 Almpandou, V., Mazaris, A.D., Mertzanis, Y., Avraam, I., Antoniou, I., Pantis, J.D., Sgardelis, S.P., 2014.
414 Providing insights on habitat connectivity for male brown bears: A combination of habitat
415 suitability and landscape graph-based models. *Ecological Modelling* 286, 37–44.
416 <https://doi.org/10.1016/j.ecolmodel.2014.04.024>
417 Bailey, L.L., Muths, E., 2019. Integrating amphibian movement studies across scales better informs
418 conservation decisions. *Biological Conservation* 236, 261–268.
419 <https://doi.org/10.1016/j.biocon.2019.05.028>

420 Bensettiti, F., Gaudillat, V., 2004. Cahiers d'habitats Natura 2000. Connaissance et gestion des habitats et
421 des espèces d'intérêt communautaire. Tome 7. Espèces animales. La Documentation française.
422 353 pp

423 Bergès, L., Avon, C., Bezombes, L., Clauzel, C., Duflot, R., Foltête, J.-C., Gaucherand, S., Girardet, X.,
424 Spiegelberger, T., 2020. Environmental mitigation hierarchy and biodiversity offsets revisited
425 through habitat connectivity modelling. *Journal of Environmental Management* 256, 109950.

426 Briers, R. A., 2002. Incorporating connectivity into reserve selection procedures. *Biological Conservation*
427 103(1), 77-83.

428 Clauzel, C., Girardet, X., Foltête, J.-C., 2013. Impact assessment of a high-speed railway line on species
429 distribution: Application to the European tree frog (*Hyla arborea*) in Franche-Comté. *Journal of*
430 *Environmental Management* 127, 125–134. <https://doi.org/10.1016/j.jenvman.2013.04.018>

431 Clauzel, C., Bannwarth, C., Foltete, J.-C., 2015. Integrating regional-scale connectivity in habitat
432 restoration: An application for amphibian conservation in eastern France. *Journal for Nature*
433 *Conservation* 23, 98–107. <https://doi.org/10.1016/j.jnc.2014.07.001>

434 Coulon, A., Aben, J., Palmer, S.C.F., Stevens, V.M., Callens, T., Strubbe, D., Lens, L., Matthysen, E.,
435 Baguette, M., Travis, J.M.J., 2015. A stochastic movement simulator improves estimates of
436 landscape connectivity. *Ecology* 96, 2203–2213. <https://doi.org/10.1890/14-1690.1>

437 Dale, M.R.T., Fortin, M.-J., 2010. From graphs to spatial graphs. *Annual Review of Ecology, Evolution, and*
438 *Systematics* 41, 21–38. <https://doi.org/10.1146/annurev-ecolsys-102209-144718>

439 Davidson, N.C., 2014. How much wetland has the world lost? Long-term and recent trends in global
440 wetland area. *Marine and Freshwater Research* 65, 934–941.

441 Decout, S., Manel, S., Miaud, C., Luque, S., 2012. Integrative approach for landscape-based graph
442 connectivity analysis: a case study with the common frog (*Rana temporaria*) in human-dominated
443 landscapes. *Landscape Ecology* 27, 267–279. <https://doi.org/10.1007/s10980-011-9694-z>

444 Duflot, R., Avon, C., Roche, P., Bergès, L., 2018. Combining habitat suitability models and spatial graphs for
445 more effective landscape conservation planning: An applied methodological framework and a
446 species case study. *Journal for Nature Conservation* 46, 38–47.
447 <https://doi.org/10.1016/j.jnc.2018.08.005>

448 Ermgassen, S.O.S.E. zu, Baker, J., Griffiths, R.A., Strange, N., Struebig, M.J., Bull, J.W., 2019. The ecological
449 outcomes of biodiversity offsets under “no net loss” policies: A global review. *Conservation*
450 *Letters* 12, e12664. <https://doi.org/10.1111/conl.12664>

451 Fall, A., Fortin, M.-J., Manseau, M., O'Brien, D., 2007. Spatial Graphs: Principles and Applications for
452 Habitat Connectivity. *Ecosystems* 10, 448–461. <https://doi.org/10.1007/s10021-007-9038-7>

453 Foltête, J.-C., 2019. How ecological networks could benefit from landscape graphs: A response to the
454 paper by Spartaco Gippoliti and Corrado Battisti. *Land Use Policy* 80, 391–394.
455 <https://doi.org/10.1016/j.landusepol.2018.04.020>

456 Foltête, J.C., Clauzel, C., Vuidel, G., 2012. A software tool dedicated to the modelling of landscape
457 networks. *Environmental Modelling & Software* 38, 316-327

458 Foltête, J.-C., Savary, P., Clauzel, C., Bourgeois, M., Girardet, X., Saharoui, Y., Vuidel, G., Garnier, S., 2020.
459 Coupling landscape graph modeling and biological data: a review. *Landscape Ecol* 1–18.
460 <https://doi.org/10.1007/s10980-020-00998-7>

461 Fourcade, Y., Engler, J.O., Rödder, D., Secondi, J., 2014. Mapping Species Distributions with MAXENT Using
462 a Geographically Biased Sample of Presence Data: A Performance Assessment of Methods for
463 Correcting Sampling Bias. *PLoS One* 9. <https://doi.org/10.1371/journal.pone.0097122>

464 Galpern, P., Manseau, M., Fall, A., 2011. Patch-based graphs of landscape connectivity: A guide to
465 construction, analysis and application for conservation. *Biological Conservation* 144, 44–55.
466 <https://doi.org/10.1016/j.biocon.2010.09.002>

467 Godet, L., Devictor, V., 2018. What Conservation Does. *Trends in Ecology & Evolution* 33, 720–730.
468 <https://doi.org/10.1016/j.tree.2018.07.004>

469 Grand, D., Boudot, J.-P., Doucet, G., 2014. Cahier d'identification des libellules de France, Belgique,
470 Luxembourg et Suisse. Biotope, Mèze, (Collection Cahier d'identification), 136p

471 Grant, E.H.C., Muths, E., Schmidt, B.R., Petrovan, S.O., 2019. Amphibian conservation in the
472 Anthropocene. *Biological Conservation* 236, 543–547.
473 <https://doi.org/10.1016/j.biocon.2019.03.003>

474 Guisan, A., Zimmermann, N.E., 2000. Predictive habitat distribution models in ecology. *Ecological*
475 *modelling* 135, 147–186.

476 Hanski, I., & Ovaskainen, O., 2000. The metapopulation capacity of a fragmented landscape. *Nature*.
477 404(6779), 755-758.

478 Hayes, T.B., Falso, P., Gallipeau, S., Stice, M., 2010. The cause of global amphibian declines: a
479 developmental endocrinologist’s perspective. *J Exp Biol* 213, 921–933.
480 <https://doi.org/10.1242/jeb.040865>

481 Hodgson, J.A., Moilanen, A., Wintle, B.A., Thomas, C.D., 2011. Habitat area, quality and connectivity:
482 striking the balance for efficient conservation. *Journal of Applied Ecology* 48, 148–152.

483 Howard, S.D., Bickford, D.P., 2014. Amphibians over the edge: silent extinction risk of Data Deficient
484 species. *Diversity and Distributions* 20, 837–846. <https://doi.org/10.1111/ddi.12218>

485 IAU, 2019. L’inventaire numérique de l’occupation du sol de l’Île-de-France.
486 <https://www.institutparisregion.fr/mode-doccupation-du-sol-mos.html>

487 Jeliakov, A., Lorrillière, R., Besnard, A., Garnier, J., Silvestre, M., Chiron, F., 2019. Cross-scale effects of
488 structural and functional connectivity in pond networks on amphibian distribution in agricultural
489 landscapes. *Freshwater Biology* 64, 997–1014.

490 Jolliffe, I.T., 2002. *Principal Component Analysis*. 2nd ed. New York: Springer-Verlag.

491 Kaiser, H. F., 1961. A Note on Guttman’s Lower Bound for the Number of Common Factors. *Br. J. Stat.*
492 *Psychol.* 14, 1–2.

493 Karger, D.N., Conrad, O., Böhrer, J., Kawohl, T., Kreft, H., Soria-Auza, R.W., Zimmermann, N.E., Linder,
494 H.P., Kessler, M., 2017. Climatologies at high resolution for the earth’s land surface areas.
495 *Scientific Data*. 4,170122

496 Khosravi, R., Hemami, M.-R., Cushman, S.A., 2018. Multispecies assessment of core areas and connectivity
497 of desert carnivores in central Iran. *Diversity and Distributions* 24, 193–207.
498 <https://doi.org/10.1111/ddi.12672>

499 Kramer-Schadt, S., Niedballa, J., Pilgrim, J.D., Schröder, B., Lindenborn, J., Reinfelder, V., Stillfried, M.,
500 Heckmann, I., Scharf, A.K., Augeri, D.M., Cheyne, S.M., Hearn, A.J., Ross, J., Macdonald, D.W.,
501 Mathai, J., Eaton, J., Marshall, A.J., Semiadi, G., Rustam, R., Bernard, H., Alfred, R., Samejima, H.,
502 Duckworth, J.W., Breitenmoser-Wuersten, C., Belant, J.L., Hofer, H., Wilting, A., 2013. The
503 importance of correcting for sampling bias in MaxEnt species distribution models. *Diversity and*
504 *Distributions* 19, 1366–1379. <https://doi.org/10.1111/ddi.12096>

505 Lechner, A.M., Sprod, D., Carter, O., Lefroy, E.C., 2017. Characterising landscape connectivity for
506 conservation planning using a dispersal guild approach. *Landscape Ecol* 32, 99–113.
507 <https://doi.org/10.1007/s10980-016-0431-5>

508 Lescure J., de Massary J.C., 2012. *Atlas des amphibiens et des reptiles de France*. Ouvrage collectif de la
509 société herpétologique de France. Biotope, Mèze ; Muséum National d’Histoire Naturelle, Paris
510 (Collection Inventaires & biodiversité), 272 p

511 Liu, C., White, M., Newell, G., 2013. Selecting thresholds for the prediction of species occurrence with
512 presence-only data. *Journal of biogeography* 40, 778–789.

513 Matos, C., Petrovan, S.O., Wheeler, P.M., Ward, A.I., 2019. Landscape connectivity and spatial
514 prioritization in an urbanising world: A network analysis approach for a threatened amphibian.
515 *Biological Conservation* 237, 238–247. <https://doi.org/10.1016/j.biocon.2019.06.035>

516 Metz, M., Rocchini, D., Neteler, M., 2014. Surface temperatures at the continental scale: Tracking changes
517 with remote sensing at unprecedented detail. *Remote Sensing* 6(5), 3822-3840

518 Meurant, M., Gonzalez, A., Doxa, A., Albert, C.H., 2018. Selecting surrogate species for connectivity
519 conservation. *Biological Conservation* 227, 326–334.
520 <https://doi.org/10.1016/j.biocon.2018.09.028>

521 Mimet, A., Clauzel, C., Foltête, J.-C., 2016. Locating wildlife crossings for multispecies connectivity across
522 linear infrastructures. *Landscape Ecology* 31, 1955–1973. [https://doi.org/10.1007/s10980-016-](https://doi.org/10.1007/s10980-016-0373-y)
523 0373-y

524 Minor, E.S., Urban, D.L., 2008. A graph-theory framework for evaluating landscape connectivity and
525 conservation planning. *Conservation Biology* 22, 297–307. [https://doi.org/10.1111/j.1523-](https://doi.org/10.1111/j.1523-1739.2007.00871.x)
526 1739.2007.00871.x

527 Moilanen, A., Franco, A. M., Early, R. I., Fox, R., Wintle, B., & Thomas, C. D., 2005. Prioritizing multiple-use
528 landscapes for conservation: methods for large multi-species planning problems. *Proceedings of*
529 *the Royal Society B: Biological Sciences* 272(1575), 1885–1891

530 Moilanen, A., 2011. On the limitations of graph-theoretic connectivity in spatial ecology and conservation.
531 *Journal of Applied Ecology* 48, 1543–1547. <https://doi.org/10.1111/j.1365-2664.2011.02062.x>

532 Moilanen, A., Kotiaho, J.S., 2018. Fifteen operationally important decisions in the planning of biodiversity
533 offsets. *Biological Conservation* 227, 112–120. <https://doi.org/10.1016/j.biocon.2018.09.002>

534 Peres-Neto, Pedro R., Donald A. Jackson, and Keith M. Somers., 2005. “How Many Principal Components?
535 Stopping Rules for Determining the Number of Non-Trivial Axes Revisited.” *British Journal of*
536 *Statistical Psychology* 49: 974–97.

537 Phillips, S.J., Anderson, R.P., Schapire, R.E., 2006. Maximum entropy modeling of species geographic
538 distributions. *Ecological modelling* 190, 231–259.

539 Phillips, S.J., Dudík, M., 2008. Modeling of species distributions with Maxent: new extensions and a
540 comprehensive evaluation. *Ecography* 31, 161–175. [https://doi.org/10.1111/j.0906-](https://doi.org/10.1111/j.0906-7590.2008.5203.x)
541 7590.2008.5203.x

542 Phillips, S.J., Anderson, R.P., Dudík, M., Schapire, R.E., Blair, M.E., 2017. Opening the black box: an open-
543 source release of Maxent. *Ecography* 40, 887–893. <https://doi.org/10.1111/ecog.03049>

544 Pittman, S.E., Osbourn, M.S., Semlitsch, R.D., 2014. Movement ecology of amphibians: A missing
545 component for understanding population declines. *Biological Conservation* 169, 44–53.
546 <https://doi.org/10.1016/j.biocon.2013.10.020>

547 Rayfield, B., Fortin, M.-J., Fall, A., 2011. Connectivity for conservation: a framework to classify network
548 measures. *Ecology* 92, 847–858. <https://doi.org/10.1890/09-2190.1>

549 Sahraoui, Y., Foltête, J.-C., Clauzel, C., 2017. A multi-species approach for assessing the impact of land-
550 cover changes on landscape connectivity. *Landscape Ecology* 32, 1819–1835.
551 <https://doi.org/10.1007/s10980-017-0551-6>

552 Santini, L., Saura, S., Rondinini, C., 2016. A Composite Network Approach for Assessing Multi-Species
553 Connectivity: An Application to Road Defragmentation Prioritisation. *PLOS ONE* 11, e0164794.
554 <https://doi.org/10.1371/journal.pone.0164794>

555 Saura, S., Estreguil, C., Mouton, C., Rodríguez-Freire, M., 2011. Network analysis to assess landscape
556 connectivity trends: Application to European forests (1990–2000). *Ecological Indicators* 11, 407–
557 416. <https://doi.org/10.1016/j.ecolind.2010.06.011>

558 Schank, C.J., Cove, M.V., Arima, E.Y., Brandt, L.S., Brenes-Mora, E., Carver, A., Diaz-Pulido, A., Estrada, N.,
559 Foster, R.J., Godínez-Gómez, O., 2020. Population status, connectivity, and conservation action
560 for the endangered Baird’s tapir. *Biological Conservation* 245, 108501.

561 Schmidt, B.R., Arletta, R., Schaub, M., Lüscher, B., Kröpfl, M., 2019. Benefits and limits of comparative
562 effectiveness studies in evidence-based conservation. *Biological Conservation* 236, 115–123.
563 <https://doi.org/10.1016/j.biocon.2019.05.033>

564 Scroggie, M.P., Preece, K., Nicholson, E., McCarthy, M.A., Parris, K.M., Heard, G.W., 2019. Optimizing
565 habitat management for amphibians: From simple models to complex decisions. *Biological*
566 *Conservation* 236, 60–69. <https://doi.org/10.1016/j.biocon.2019.05.022>

567 Smith, M., Green, D., 2005. Dispersal and the metapopulation paradigm in amphibian ecology and
568 conservation: are all amphibian populations metapopulations? *Ecography* 28, 110–128.
569 <https://doi.org/10.1111/j.0906-7590.2005.04042.x>

570 Sordello, R., Comolet-Tirman, J., De Massary, J.-C., Dupont, P., Haffner, P., Rogeon, G., Siblet, J.-P.,
571 Tourroult, J., Trouvilliez, J., 2011. *Trame verte et bleue. Critères nationaux de cohérence.*

572 *Contribution à la définition du critère sur les espèces*. Rapport d'étude No. SPN 2011-21. Service
573 du Patrimoine Naturel, Muséum National d'Histoire Naturelle.

574 Urban, D.L., Minor, E.S., Treml, E.A., Schick, R.S., 2009. Graph models of habitat mosaics. *Ecology Letters*
575 12, 260–273. <https://doi.org/10.1111/j.1461-0248.2008.01271.x>

576 Verbeylen G., De Bruyn L., Adriaensen F., Matthysen E., 2003. Does matrix resistance influence Red
577 squirrel (*Sciurus vulgaris* L. 1758) distribution in an urban landscape? *Landscape Ecology* 18, 791–
578 805.

579 Wilson, J.W., Sexton, J.O., Jobe, R.T., Haddad, N.M., 2013. The relative contribution of terrain, land cover,
580 and vegetation structure indices to species distribution models. *Biological Conservation* 164, 170–
581 176.

582 Ziólkowska, E., Ostapowicz, K., Kuemmerle, T., Perzanowski, K., Radeloff, V.C., Kozak, J., 2012. Potential
583 habitat connectivity of European bison (*Bison bonasus*) in the Carpathians. *Biological conservation*
584 146, 188–196.

585 Zucca M., Loïs G., Muratet A., Ricci O., 2019. Panorama de la biodiversité francilienne. ARB ÎdF, Paris

586

587

588

589 **Appendices**

590
 591 Appendix A: Resistance values assigned to each category of the landscape map for each species, based on
 592 information from the literature.
 593

Species	Forest edges	Forests	Open shrubby environments	Grasslands	Crops	Quarries	Urban green environments	Artificial environments	Major roads	Minor roads	Buildings	Small rivers	Surface waters	Large rivers	Ponds
<i>Alytes obstetricans</i>	10	100	10	10	100	10	10	100	10000	1000	10000	10	10	100	1
<i>Bufo bufo</i>	10	10	10	100	100	1000	100	100	10000	1000	10000	100	1	1000	1
<i>Epidalea calamita</i>	100	1000	10	10	100	10	100	100	10000	1000	10000	10	10	100	1
<i>Hyla arborea</i>	10	100	10	10	1000	1000	100	1000	10000	1000	10000	10	10	100	1
<i>Natrix natrix</i>	10	100	10	10	1000	100	1000	1000	10000	1000	10000	10	1	100	1
<i>Rana temporaria</i>	10	10	10	10	100	100	100	10	10000	100	10000	10	1	1000	1
<i>Salamandra salamandra</i>	10	10	100	100	1000	1000	100	1000	10000	1000	10000	10	10	100	1
<i>Triturus cristatus</i>	10	10	10	10	1000	100	100	100	10000	1000	10000	10	10	1000	1

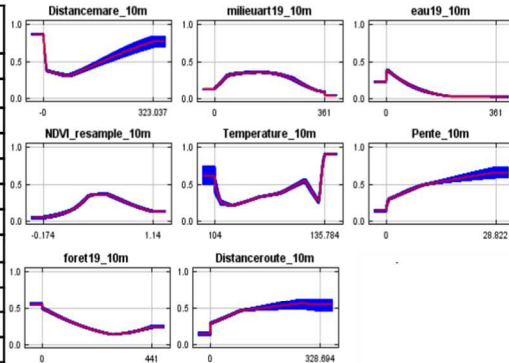
594
 595
 596
 597
 598 Appendix B: Results of the average accuracy of the predictive models for the 8 species using Maxent. AUC
 599 = area under the curves of relative operational characteristics. The results of the threshold "maximum test
 600 sensitivity plus specificity" = max SSS and the extrinsic omission rate (proportion of test localities not
 601 included in the prediction) are given for each of the 10 random data partitions. For all 8 species, the
 602 binomial test was highly significant for all partitions ($p < 0.001$, one-sided).

	AUC	Max SSS	Percentage of habitat area
<i>Alytes obstetricans</i>	0.902 +/- 0.012	0.24	11.62%
<i>Bufo bufo</i>	0.843 +/- 0.008	0.33	11.03%
<i>Epidalea calamita</i>	0.955 +/- 0.013	0.16	4.55%
<i>Hyla arborea</i>	0.940 +/- 0.016	0.18	8.31%
<i>Natrix natrix</i>	0.900 +/- 0.015	0.24	15.13%
<i>Rana temporaria</i>	0.839 +/- 0.009	0.32	15.30%
<i>Triturus cristatus</i>	0.951 +/- 0.006	0.13	8.48%
<i>Salamandra salamandra</i>	0.976 +/- 0.025	0.25	0.55%

603
 604
 605
 606 Appendix C: List of the contributive variables and Maxent response curves for the variables that
 607 contributed the most (> 2%) for each of the eight pond-dwelling species.

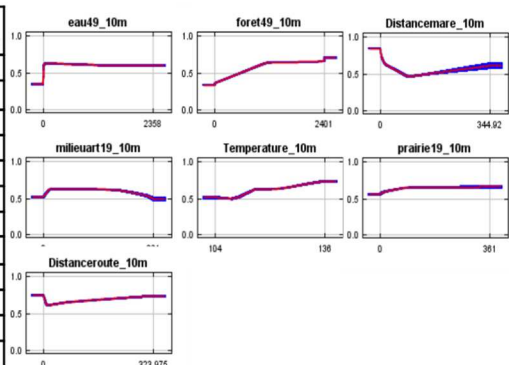
Alytes obstetricans

Variable	Percent contribution
Distancemare	34.4
milieuart19	24.2
eau19	15.7
NDVI	6.4
Temperature	5.6
Pente	3.5
foret19	2.4
Distanceroute	2.1
Distanceeau	1.8
prairie19	1.6
Precipitations	1.6
carriere5	0.7



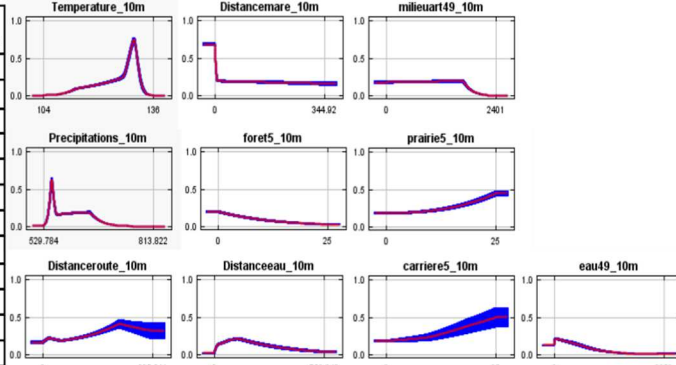
Bufo bufo

Variable	Percent contribution
eau49	51
foret49	18.6
Distancemare	12.7
milieuart19	6.7
Temperature	3
prairie19	2.7
Distanceroute	2
Distanceeau	1.2
eau5	0.9
Precipitations	0.7
NDVI	0.2
Pente	0.2



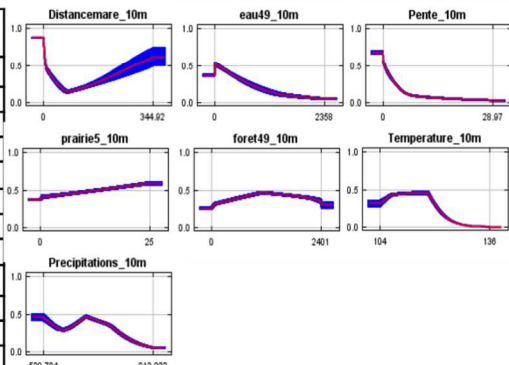
Epidalea calamita

Variable	Percent contribution
Temperature	32.1
Distancemare	22
milieuart49	14.8
Precipitations	8.6
foret5	5.4
prairie5	5
Distanceroute	3.4
Distanceeau	2.9
carriere5	2.5
eau49	2.1
NDVI	0.9
Pente	0.3



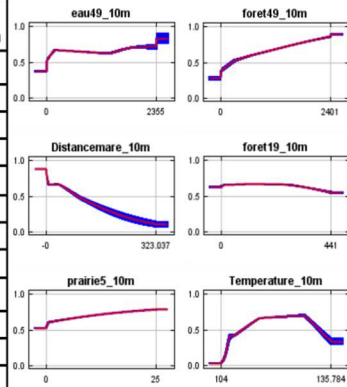
Hyla arborea

Variable	Percent contribution
Distancemare	44.6
eau49	20.9
Pente	8.4
prairie5	7.8
foret49	5.8
Temperature	3.7
Precipitations	2.3
milieuart49	1.9
NDVI	1.9
Distanceroute	1.7
Distanceeau	0.6
carriere49	0.4



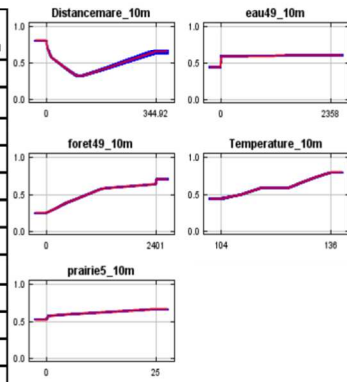
Natrix natrix

Variable	Percent contribution
eau49	36.5
foret49	16.9
Distancemare	15
foret19	9.4
prairie5	7.9
Temperature	6.5
Distanceeau	1.7
NDVI	1.6
milieuart49	1.5
Precipitations	1.4
Distanceroute	1.1
Pente	0.4



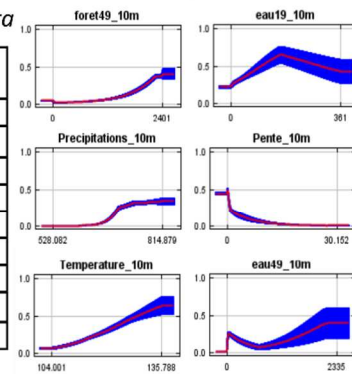
Rana temporaria

Variable	Percent contribution
Distancemare	33
eau49	30.8
foret49	27.7
Temperature	2.9
prairie5	2
Precipitations	1.3
milieuart5	0.8
Distanceroute	0.4
Pente	0.4
Distanceeau	0.3
NDVI	0.3
carriere19	0.1



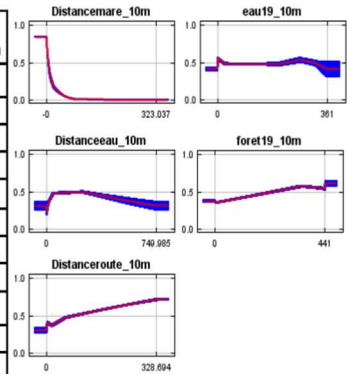
Salamandra salamandra

Variable	Percent contribution
foret49	30.5
eau49	23.9
Precipitations	17.4
Pente	13.1
Temperature	6
eau19	5.3
prairie49	1.8
NDVI	1.5
Distanceeau	0.5



Triturus cristatus

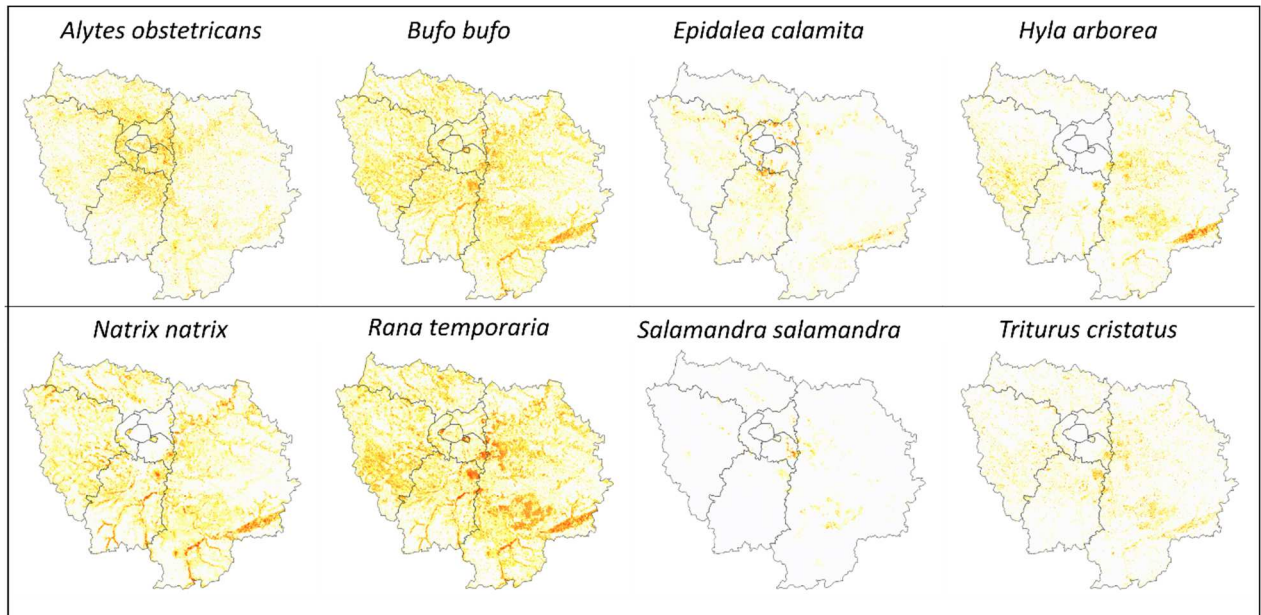
Variable	Percent contribution
Distancemare	69.5
eau19	13
Distanceeau	4.3
foret19	3
Distanceroute	2.1
milieuart49	1.8
prairie5	1.7
Temperature	1.6
Precipitations	1.2
Pente	1.2
NDVI	0.6



609

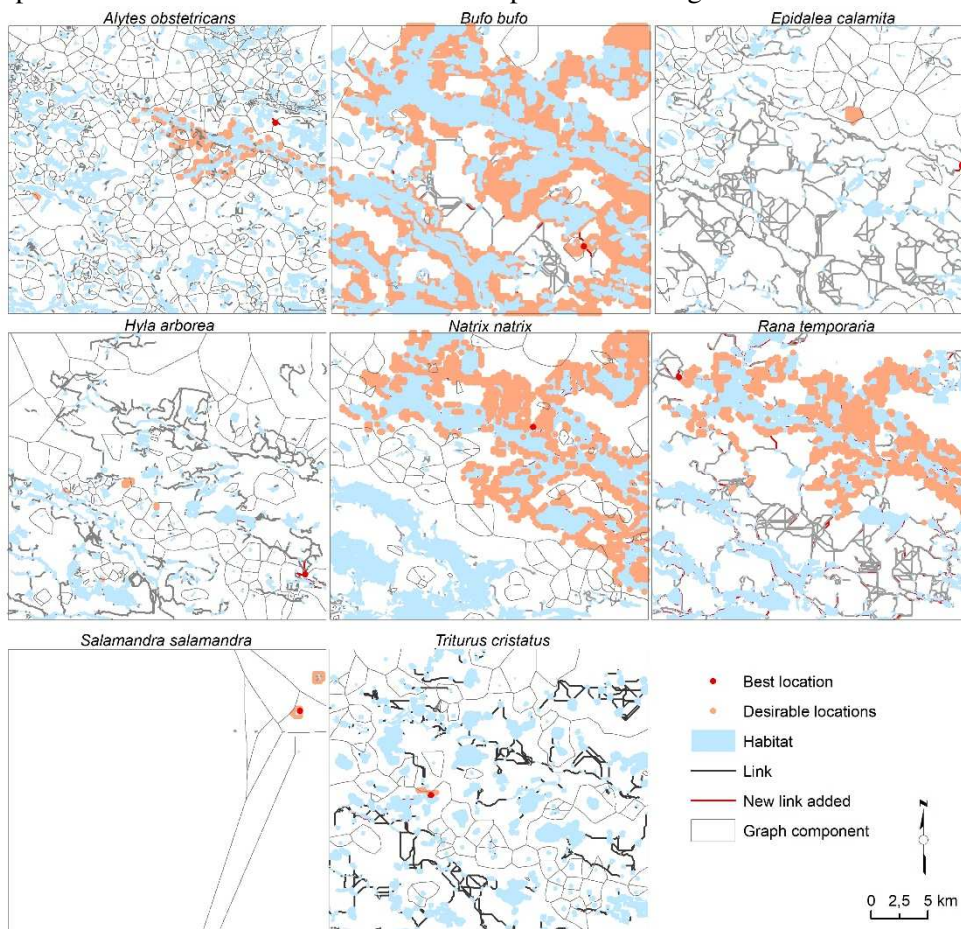
610

611 Appendix D: Habitat suitability models (HSM) corresponding to each species (red = highest probability of
 612 presence; white: zero probability of presence)



613
 614
 615
 616
 617
 618
 619

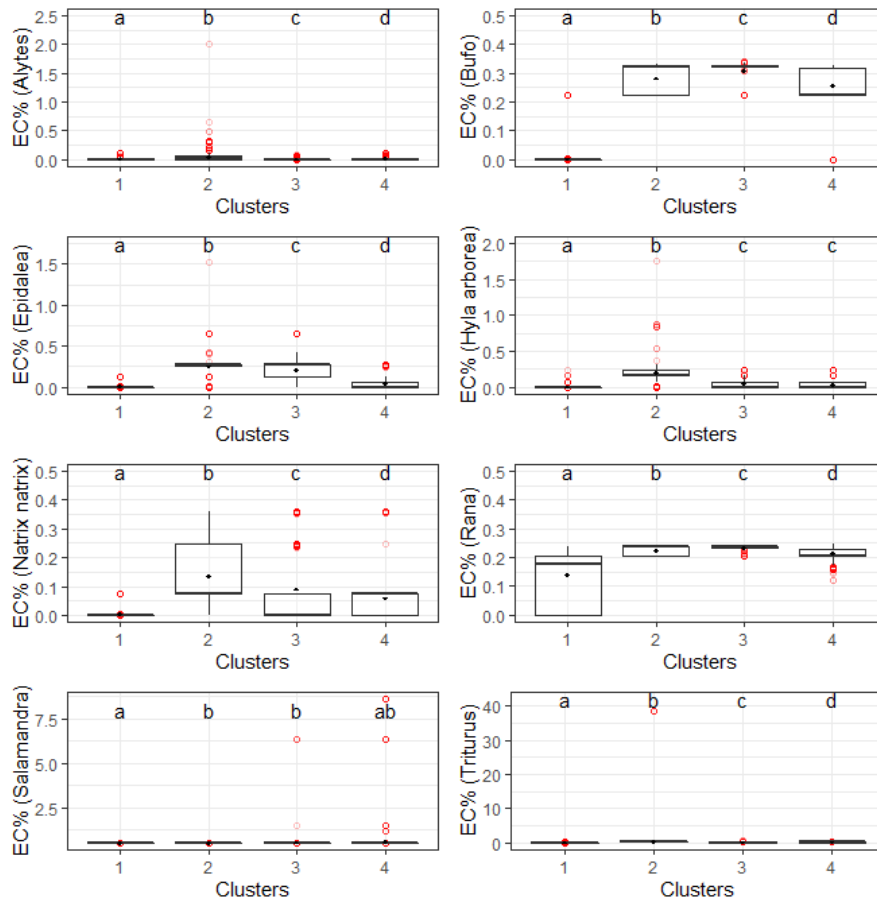
Appendix E: Landscape graphs representing the ecological network of each species and the best locations
 for adding a new pond according to the gain in connectivity. The desirable locations corresponded to the
 class with the highest increase in the Equivalent Connectivity (EC) metric. Their number varied according
 to species. The best location was the one that provided the highest increase.



620

621
 622 Appendix F: Boxplots of the values of the percentage increase in the EC metric for each species. The
 623 outliers are in red. Following the Wilcoxon post hoc tests, the letters (a, b, c, and d) corresponded to the
 624 representation of significance. If two clusters have the same letter, then they are not significantly different
 625 and vice-versa.

626



627

628